

*Electronic Supporting Information (ESI)*

**Improving hydrogen selectivity of graphene oxide membranes by  
reducing non-selective pores with intergrown ZIF-8 crystals**

Xuerui Wang,<sup>a</sup> Chenglong Chi,<sup>a</sup> Jifang Tao,<sup>b</sup> Yongwu Peng,<sup>a</sup> Shaoming Ying,<sup>a</sup> Yuhong Qian,<sup>a</sup> Jinqiao Dong,<sup>a</sup> Zhigang Hu,<sup>a</sup> Yuandong Gu<sup>b</sup> and Dan Zhao<sup>a\*</sup>

<sup>a</sup> Department of Chemical & Biomolecular Engineering, National University of Singapore, 4 Engineering Drive 4, 117585 Singapore

<sup>b</sup> Institute of Microelectronics, A\*STAR (Agency for Science, Technology and Research), 11 Science Park Road, 117685 Singapore

Correspondence and requests for materials should be addressed to D.Z. (E-mail: [chezhao@nus.edu.sg](mailto:chezhao@nus.edu.sg)).

## Experimental Section

**Exfoliation of GO nanosheets:** Few-layered GO nanosheets (Figure S1) were exfoliated by freeze-thaw approach as reported in our previous study.<sup>[1]</sup> To be specific, the bulk GO powder (Nanjing XFNANO Materials Tech Co.) dispersed in deionized water with a concentration of  $0.5 \text{ mg}\cdot\text{mL}^{-1}$  was quickly frozen in liquid nitrogen and then thawed in boiling water. After 6 cycles of freeze-thaw, the suspension became almost homogeneous brown solution and then was centrifuged at 4000 rpm for 30 min to remove the unexfoliated and aggregated large GO particles. The supernatant was collected and further purified by pH-assisted selective sedimentation.<sup>[2]</sup> The pH value was adjusted to 3.0-4.0 using 1 M HCl. After free-standing for over 4 h, the upper dispersion was removed. The residual bottom dispersion was collected and diluted with deionized water affording GO nanosheet stock solution for membrane preparation.

**Preparation of ultrathin GO and rGO membranes:** the GO membrane was prepared by vacuum filtrating GO stock solution (5 mL) onto an asymmetric  $\alpha\text{-Al}_2\text{O}_3$  disk substrate (Inoceramic), which has a top layer pore size of 70 nm. The as-prepared GO membrane was dried in vacuum oven for 24 h at  $40^\circ\text{C}$  for further usage. Reduced GO (rGO) membrane was prepared by reducing the as-prepared GO membrane with hydrazine hydrate vapor at  $140^\circ\text{C}$  for 6 h according to a published procedure.<sup>[3]</sup> Briefly, the as-prepared GO membrane was sealed by silicon rubber and mounted in a stainless steel cell, which was placed in a temperature-controlled furnace. A hydrogen stream saturated with hydrazine hydrate vapor was introduced onto one side of the GO membrane (feed side), while the other side of the GO membrane (permeate side) was swept by argon. Both sides of the membrane were maintained at atmospheric pressure.

**Modification of GO membranes with intergrown ZIF-8 crystals:** The zinc salt stock solution was prepared by dissolving 0.11 g (18.1 mmol) of  $\text{Zn}(\text{NO}_3)_2\cdot 6\text{H}_2\text{O}$  in 20 mL of deionized water. The organic ligand stock solution was prepared by dissolving 2.27 g (1.4 mol) of 2-methylimidazole in 20 mL of deionized water. The zinc solution was added dropwise onto a horizontally placed GO membrane over a period of 60 min. After that, the GO membrane was rinsed with deionized water and soaked into the ligand solution overnight. The as-modified GO membrane was rinsed with deionized water and dried under ambient conditions for further usage. For a comparison of membrane modification with unlimited zinc and ligand source, the as-synthesized GO membrane was directly soaked in zinc and ligand mixed solution (1:1) for 6 h.

**Characterization:** The size and height of GO nanosheets were observed at room temperature by atomic force microscopy (AFM, Bruker Dimension ICON) in tapping mode with a silicon cantilever with force constant of  $10\text{-}130 \text{ N m}^{-1}$ . Analysis of the AFM images was performed using the NanoScope Analysis. The morphology of GO nanosheets and the membrane was observed by transmission electron microscopy (TEM) and field emission scanning electron microscopy (FE-SEM, JSM-7610F, JEOL). Prior to focused-ion-beam (FIB) cutting, the GO layer was sandwiched between the FIB-deposited platinum (to protect the coating from milling) and the alumina support. The crystal phase of ZIF-8 on the surface of GO membrane was measured by powder X-ray diffraction (PXRD, MiniFlex 600, Rigaku) equipped with a Cu sealed tube ( $\lambda = 0.154178 \text{ nm}$ ) with a scan rate of  $0.02 \text{ deg}\cdot\text{s}^{-1}$ . X-ray photoelectron spectroscopy (XPS) measurements were performed using a Kratos AXIS Ultra (Kratos Analytical Ltd) with a monochromated Al  $\text{K}_\alpha$  radiation ( $h\nu = 1486.6 \text{ eV}$ ). The water removal from membranes was confirmed by mass

spectrometry. Briefly, the supported membrane was heated in a tube furnace from room temperature to 160 °C at a heating rate of 0.5 °C·min<sup>-1</sup> under the presence of Ar as the sweep gas (5 mL·min<sup>-1</sup>). Then, the temperature was kept at 160 °C until the water was completely removed. A mass spectrometer (Hiden QGA) was connected to the tube furnace to detect the signal of released water.

**Gas permeation tests:** All the gas permeation tests were performed in a home-built Wicke-Kallenbach gas permeation apparatus under atmospheric pressure. Argon was used as the sweep gas at the permeate side. The permeate stream was analyzed on-line by a gas chromatography (Shimadzu GC-2014). Prior to gas permeation test, the edge of the membrane was masked with aluminum foil/glass cloth tape (3M Company) to protect the GO layer from direct contact with the silicone rubber pad. The diameter of the effective membrane area for testing was 10 mm. For the single gas permeation tests, the flow rates for feed and sweep gas were both 25 mL·min<sup>-1</sup>, which were regulated by mass flow controllers (Brooks Instrument). For the binary mixed gas separation tests, the feed flow rate of each gas was kept at 12.5 mL·min<sup>-1</sup>. The two gases were well-mixed in a chamber before entering the feed side of the membrane cell. The flow rate of sweep gas (Ar) was kept constant at 25 mL·min<sup>-1</sup>. The gas permeance ( $P_i$ , GPU) and permselectivity for hydrogen to other gases ( $S_{H_2/i}$ ) are calculated by

$$P_i = \frac{J_i}{3.3928 \times 10^{-10} \Delta P_i}$$

$$S_{H_2/i} = \frac{J_{H_2}}{J_i}$$

where  $J_i$  is permeation flux through membrane, mol·m<sup>-2</sup>·s<sup>-1</sup>;  $\Delta P_i$  is the transmembrane pressure difference of component  $i$ , Pa.

The separation factor ( $\alpha_{i/j}$ ) is calculated by

$$\alpha_{i/j} = \frac{y_i/y_j}{x_i/x_j}$$

where  $x_i$  and  $x_j$  are the molar fractions of component  $i$  and component  $j$  for the feed, respectively;  $y_i$  and  $y_j$  are the corresponding molar fractions in the permeate.

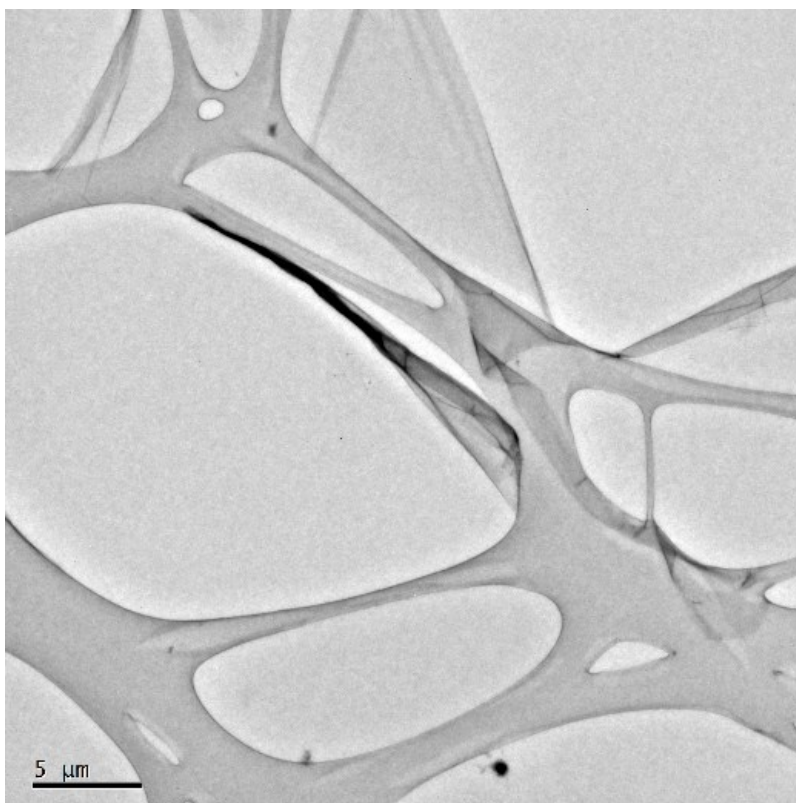


Figure S1 TEM image of exfoliated few-layered GO nanosheets.

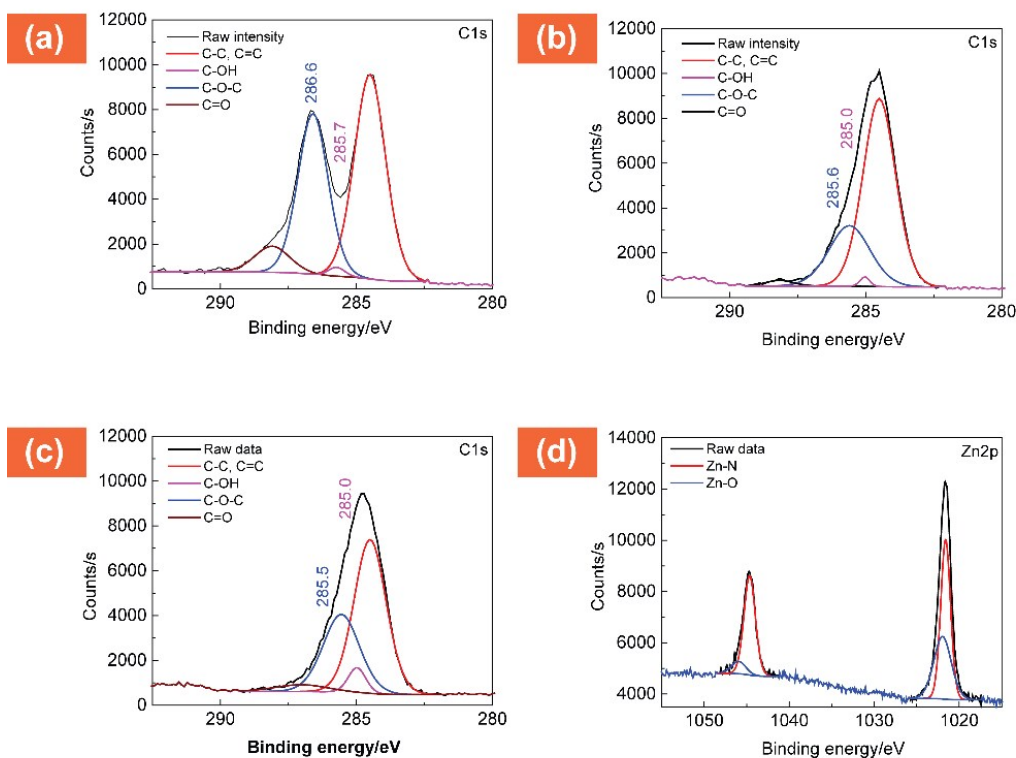


Figure S2 XPS spectra of (a) pristine GO membrane, (b) GO membrane anchored with Zn<sup>2+</sup> ions, and (c-d) GO membrane intergrown with ZIF-8.

For pristine GO membrane, two obvious peaks are observed from the C1s spectrum as shown in Figure S2a. The deconvolution displays four peaks located at binding energies of 284.5, 285.7, 286.6 and 288.1 eV, which can be assigned to the graphitic (*e.g.*, C-C and C=C), hydroxyl (C-OH), epoxide (C-O-C) and carbonyl (C=O) groups, respectively.<sup>[3, 4]</sup> The C/O ratio of our GO membrane is 3.6, indicating abundant amount of oxygen-containing groups for anchoring Zn cations. As expected, the binding energies of these oxygen-containing functional groups largely decrease after coordinating with Zn cations. For example, the binding energy for C-OH groups decrease from 285.7 to 285.0 eV (Figure S2b-c). To further confirm the presence of coordination bonds between Zn cations and GO membrane, Zn 2p XPS spectra were taken for ZIF-8 modified GO membrane. As shown in Figure S2d, the peak can be fitted to two peaks with the binding energy of 1021.5 and 1021.8 eV, respectively. The first peak can be assigned to the Zn-N bonds, and the second peak corresponds to Zn-O bonds. These results indicate that the Zn cations can be anchored by the oxygen-containing functional groups of GO acting as nucleation sites for ZIF-8 growth.

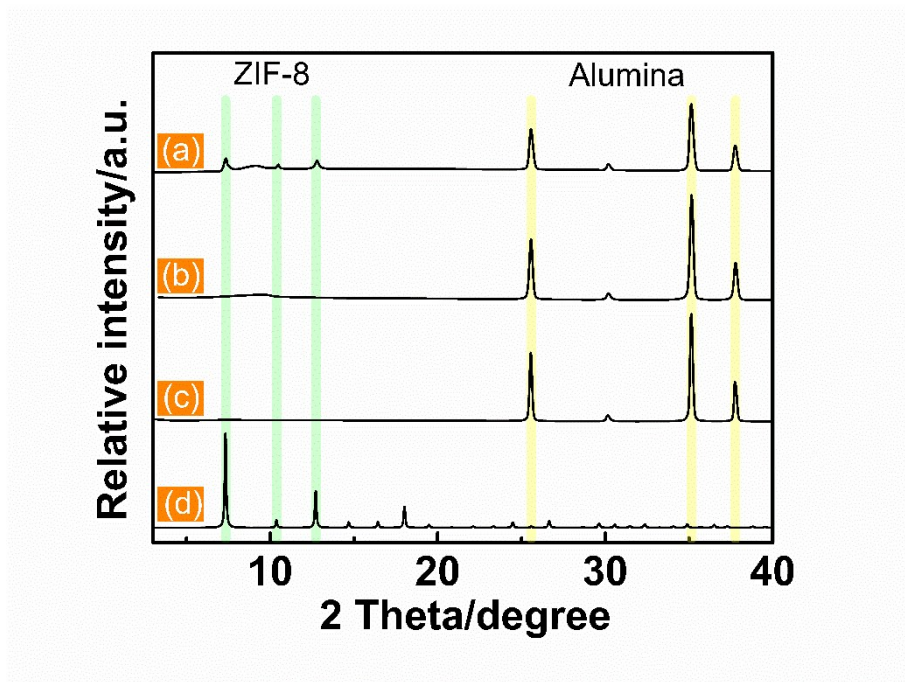


Figure S3 PXRD patterns of (a) ZIF-8 modified GO membrane, (b) pristine GO membrane, (c) alumina substrate and (d) simulated ZIF-8.

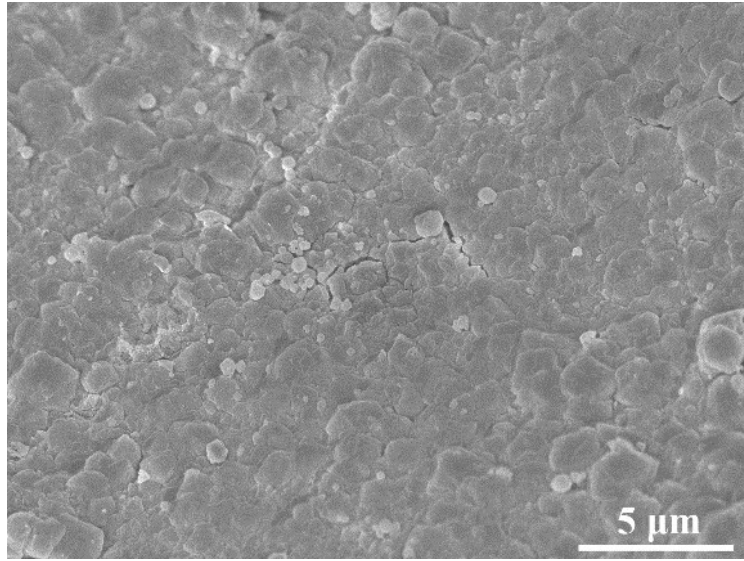


Figure S4 SEM image of a continuous ZIF-8 layer on GO membrane obtained in the compare experiment.

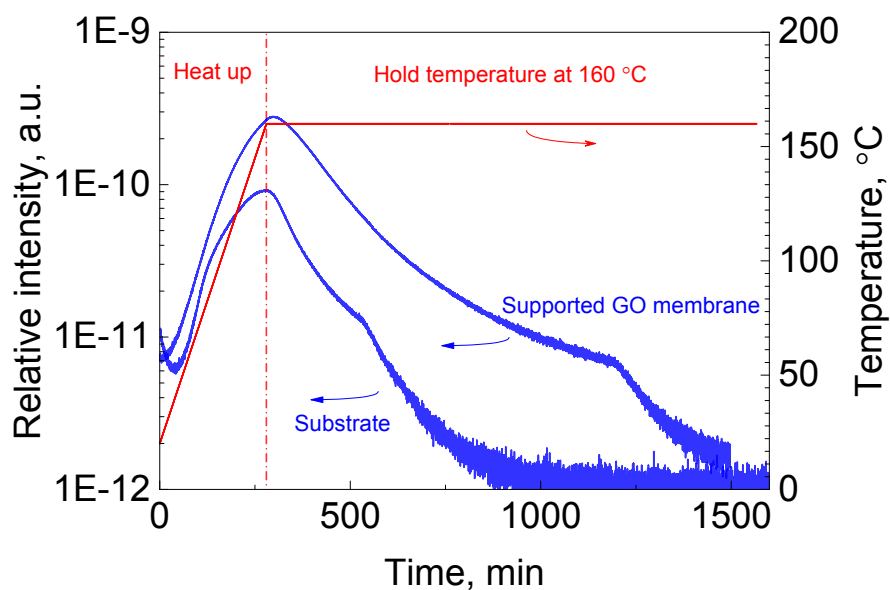


Figure S5 H<sub>2</sub>O signal detected by mass spectroscopy during the thermal treatment of supported GO membrane and substrate.

The release of water from GO membrane layer was confirmed by on line mass spectroscopy. As shown in Figure S5, the apparent mass spectroscopy signal of water indeed confirms the release of water from the substrate and the GO membrane layer during thermal treatment. Choi and Park *et al.* also observed the release of water from GO membrane layer at a temperature of ~ 140 °C.<sup>[5]</sup>

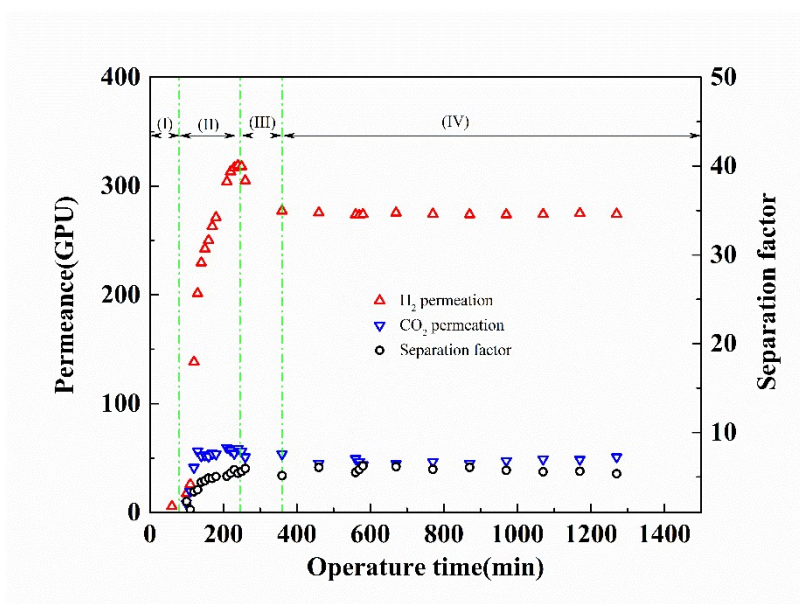


Figure S6 On-stream activation of pristine GO membrane by gas purge (I, room temperature; II, 160 °C; III, cool down to room temperature from 160 °C; IV, room temperature)

Table S1 Comparison of the gas separation performance of ZIF-8 modified GO membrane with other reported GO and ZIF-8 membranes

Membrane	Thickness	Substrate	Temp./°C	$P_{H_2}/GPU$	$\alpha_{H_2/i}$	Ref
GO	ca. 20 nm	$\alpha$ -Al <sub>2</sub> O <sub>3</sub> disk (70 nm)	25	275	H <sub>2</sub> /CO <sub>2</sub> (6.2)	This work
rGO		$\alpha$ -Al <sub>2</sub> O <sub>3</sub> disk (70 nm)	25	205	H <sub>2</sub> /CO <sub>2</sub> (5.9)	This work
ZIF-8 modified rGO		$\alpha$ -Al <sub>2</sub> O <sub>3</sub> disk (70 nm)	25	189	H <sub>2</sub> /CO <sub>2</sub> (13.6)	This work
ZIF-8 modified GO		$\alpha$ -Al <sub>2</sub> O <sub>3</sub> disk (70 nm)	25	240 218 254	H <sub>2</sub> /CO <sub>2</sub> (406) H <sub>2</sub> /N <sub>2</sub> (155) H <sub>2</sub> /CH <sub>4</sub> (355)	This work
GO	1.8-18 nm	AAO (20nm)	25	346 340	H <sub>2</sub> /CO <sub>2</sub> (3400) H <sub>2</sub> /N <sub>2</sub> (900)	Science, 2013 <sup>[6]</sup>
ZIF-8/GO	100 nm	AAO (100 nm)	25	161	H <sub>2</sub> /CO <sub>2</sub> (1.6 <sup>a</sup> ) H <sub>2</sub> /N <sub>2</sub> (11.1 <sup>a</sup> ) H <sub>2</sub> /CH <sub>4</sub> (11.2 <sup>a</sup> ) H <sub>2</sub> /C <sub>3</sub> H <sub>6</sub> (33.8 <sup>a</sup> ) H <sub>2</sub> /C <sub>3</sub> H <sub>8</sub> (405 <sup>a</sup> )	Angew. Chem. Int. Ed., 2015 <sup>[7]</sup>
ZIF-8@GO	10-20 $\mu$ m	$\alpha$ -Al <sub>2</sub> O <sub>3</sub> disk	250	374 395 380	H <sub>2</sub> /CO <sub>2</sub> (14.9) H <sub>2</sub> /N <sub>2</sub> (90.5) H <sub>2</sub> /CH <sub>4</sub> (139.1)	<i>J. Am. Chem. Soc.</i> , 2014 <sup>[8]</sup>
ZIF-8	30 $\mu$ m	TiO <sub>2</sub> disk	25	178 150	H <sub>2</sub> /CO <sub>2</sub> (4.5 <sup>a</sup> ) H <sub>2</sub> /N <sub>2</sub> (5.8 <sup>a</sup> ) H <sub>2</sub> /CH <sub>4</sub> (11.2)	<i>J. Am. Chem. Soc.</i> , 2009 <sup>[9]</sup>
ZIF-8	2 $\mu$ m	Hollow YSZ ceramic fiber	25	4539 22	H <sub>2</sub> /CO <sub>2</sub> (3.85 <sup>a</sup> ) H <sub>2</sub> /N <sub>2</sub> (11 <sup>a</sup> ) H <sub>2</sub> /CH <sub>4</sub> (13)	<i>J. Membr. Sci.</i> , 2012 <sup>[10]</sup>

<sup>a</sup>: Ideal separation factor

## Reference

- [1] C. Chi, X. Wang, Y. Peng, Y. Qian, Z. Hu, J. Dong and D. Zhao, *Chem. Mater.*, **2016**, DOI: 10.1021/acs.chemmater.5b04475.
- [2] X. Wang, H. Bai and G. Shi, *J. Am. Chem. Soc.*, 2011, **133**, 6338.
- [3] P.-G. Ren, D.-X. Yan, X. Ji, T. Chen and Z.-M. Li, *Nanotechnology*, 2011, **22**, 055705.
- [4] S. Stankovich, D. A. Dikin, R. D. Piner, K. A. Kohlhaas, A. Kleinhammes, Y. Jia, Y. Wu, S. T. Nguyen and R. S. Ruoff, *Carbon*, 2007, **45**, 1558.
- [5] H. W. Kim, H. W. Yoon, S.-M. Yoon, B. M. Yoo, B. K. Ahn, Y. H. Cho, H. J. Shin, H. Yang, U. Paik, S. Kwon, J.-Y. Choi and H. B. Park, *Science*, 2013, **342**, 91.
- [6] H. Li, Z. Song, X. Zhang, Y. Huang, S. Li, Y. Mao, H. J. Ploehn, Y. Bao and M. Yu, *Science*, 2013, **342**, 95.
- [7] Y. Hu, J. Wei, Y. Liang, H. Zhang, X. Zhang, W. Shen and H. Wang, *Angew. Chem. Int. Ed.*, 2015, **55**, 2048.
- [8] A. Huang, Q. Liu, N. Wang, Y. Zhu and J. Caro, *J. Am. Chem. Soc.*, 2014, **136**, 14686.
- [9] H. Bux, F. Liang, Y. Li, J. Cravillon, M. Wiebcke and J. Caro, *J. Am. Chem. Soc.*, 2009, **131**, 16000.
- [10] Y. C. Pan, B. Wang and Z. P. Lai, *J. Membr. Sci.*, 2012, **421**, 292.